International Journal of Pure and Applied Mathematics
Volume 99 No. 4 2015, 385-398
ISSN: 1311-8080 (printed version); ISSN: 1314-3395 (on-line version)
url: http://www.ijpam.eu
doi: http://dx.doi.org/10.12732/ijpam.v99i4.1

INVESTIGATION OF MHD FLOW STOKES PROBLEM PAST A POROUS CONTRACTING SURFACE WITH HEAT TRANSFER

Muondwe Samuel[1], Mathew Kinyanjui[2], David Theuri[3], Kangethe Giterere[4] §

[1,2,3,4]Department of Pure and Applied Mathematics
Jomo Kenyatta University of Agriculture and Technology
P.O. Box 62000, Nairobi, KENYA

Abstract: The unsteady, laminar hydro magnetic flow of an incompressible, viscous and electrically conducting Newtonian fluid over a contracting sheet embedded in a porous medium has been investigated. The flow takes place between two parallel flat sheets that are made of an electrically non-conducting material. The fluid is subjected to transverse magnetic field that cuts perpendicularly across the flow in the positive direction of the z-axis. The contracting sheet has a permeable surface while the surface of other sheet is impermeable, each sheet has an isothermal surface and both sheets are kept at different temperature of T_W andT_∞ such that the temperature differences within the flow are sufficiently small. The effect of varying various parameters on the velocity and temperature profiles has been discussed. The coupled non-linear partial differential equations governing the flow have been solved numerically using the finite difference method because of its accuracy, stability and convergence. The results that are obtained are then presented graphically and observations have been discussed. Changes in various parameters have been observed to alter the velocity profiles and temperature profiles.

AMS Subject Classification: 76D05
Key Words: contracting surface, porous media, radiation, magnetic field

1. Introduction

The study of heat transfer in the boundary layer flow has many applications in engi-

Received: March 12, 2013

§Correspondence author

neering such as in the design of thrust bearings and radial diffusers, in transpiration cooling, in drag reduction and in thermal recovery of oil. In the past most researchers have studied wide variety of flow situations. Some of these studies can be found in work of [11] studied flow and heat transfer of a fluid through a porous medium over a stretching surface with internal heat generation/ absorption and suction/ blowing. [3] investigated numerical steady free convection flow through a porous medium around a rectangular isothermal body. [10] analyzed the effects of magnetic field on the viscoelastic fluid flow and heat transfer over a non isothermal stretching sheet with internal heat generation. [16] investigated the effects of buoyancy force on the parallel flows bounded above by a rigid permeable plate which may be moving or stationary, and below, by a permeable bed. To discuss the solution, the flow region was divided into two zones: one zone made up of laminar flow and governed by Naiver Stokes equations, and the other zone was governed by Darcy's law. [1] carried out an analytical study of a two dimensional unsteady MHD free convective flow past a vertical porous plate immersed in a porous medium with hall current, thermal diffusion and heat source.

There is extensive literature on flow through porous media that is governed by generalized Darcy laws. [12] used these equations to study the influence of free convective flow and mass transfer on flow through porous medium. [13] studied thermal diffusion and chemical reaction effects on unsteady MHD free convection flow past a semi infinite vertical permeable moving plate. [6] analyzed the heat and mass transfers corresponding to the similarity for the boundary layer over a stretching sheet subjected to suction/blowing.

[8] presented work on MHD free convection heat and mass transfers of a heat generation fluid past an impulsively started infinite porous plate with Hall currents and radiation absorption. [9] analyzed effects of thermal radiation and viscous dissipation on MHD heat and mass diffusion flow past a surface embedded in porous media. [4] studied the effects of radiation, heat generation and viscous dissipation on MHD free convection flow along a stretching sheet.

Various aspect of the problem of flow over stretching surface has been studied under varied conditions. [14] studied free convective mass transfer flow past infinite vertical porous plate with variable suction and Soret effect. [2] analyzed effects of Heat source/sink on MHD flow and heat transfer over a shrinking sheet with mass suction. [15] studied Hall effects on MHD convective flow through a medium in a rotating parallel plate channel. [7] analyzed three dimensional rotating flow induced by shrinking sheet for suction. The aim of this work is therefore to study MHD Stokes fluid flow problem past a porous contracting surface with heat transfer.

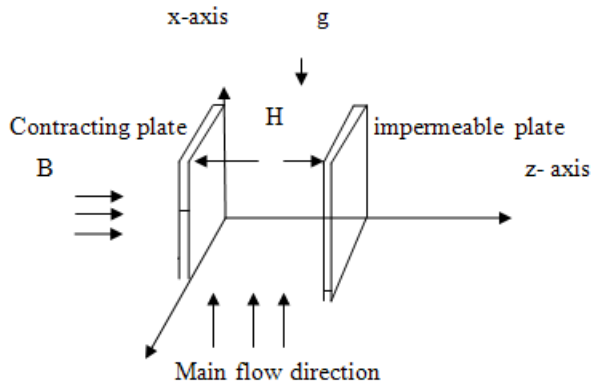

Figure 1: Flow Configuration

2. Mathematical Formulations

Consider an unsteady MHD laminar boundary layer flow of an incompressible, electrically conducting, and viscous Newtonian fluid past a contracting electrically non-conducting sheet embedded in porous media with heat transfer. The contracting sheet is permeable to allow for a possible suction and is continuously contracting in the x-axis direction in the plane $z = 0$ with a velocity $u = -cx$.

At distance H units away, a second impermeable and electrically non-conducting sheet is placed parallel to the contracting sheet. The y axis is taken to be infinite. The pressure gradient is in the positive x-axis direction, and is directed upward parallel to the direction of gravity.

The velocity vector **q** and magnetic field **B** have components (u, v, w) and (B_x, B_y, B_z) along the x, y and z-axis respectively. The fluid flows upwards against the force of gravity due to a constant pressure gradient $\frac{\partial p}{\partial x}$ transmitted to the fluid by the contracting sheet. The permeable contracting sheet is subjected to a uniform suction of magnitude ω_0.

The surface of the contracting sheet is maintained at a uniform temperature T_w. The free stream temperature is T_∞. The temperature T_w may either exceed the free stream temperature T_∞ or may be less than T_∞. When $T_w > T_\infty$ an upward flow is established along the surface due to free convection; when $T_w < T_\infty$, there is a down flow.

The equation of momentum along the x-axis is

$$\frac{\partial u}{\partial t} + u\frac{\partial u}{\partial x} + \omega_o \frac{\partial u}{\partial z} = \nu\left(\frac{\partial^2 u}{\partial x^2} + \frac{\partial^2 u}{\partial z^2}\right) - u\frac{\nu}{k_p} - \frac{\sigma u B_o^2}{\rho} + \beta g\,(T - T_\infty) \qquad (1)$$

The equation of momentum along the y – axis is

$$\frac{\partial v}{\partial t}+\frac{u\partial v}{\partial x}+\omega_o\frac{\partial v}{\partial z}=\nu\left(\frac{\partial^2 v}{\partial x^2}+\frac{\partial^2 v}{\partial z^2}\right)-\nu\frac{v}{k_p}-\frac{\sigma u B_o^2}{\rho} \tag{2}$$

The equation of energy is

$$\begin{aligned}\frac{\partial T}{\partial t}+u\frac{\partial T}{\partial x}+\omega_o\frac{\partial T}{\partial z} &= \frac{k_f}{\rho C_p}\left(\frac{\partial^2 T}{\partial x^2}+\frac{\partial^2 T}{\partial z^2}\right)+\frac{\sigma}{\rho C_p}B_0^2\left(u^2+v^2\right)\\ &\quad+\frac{\mu}{\rho C_p}\left[\left(\frac{\partial u}{\partial x}\right)^2+\left(\frac{\partial v}{\partial z}\right)^2\right]-\frac{16\sigma^* B_o^2}{3\rho C_p k^*}\frac{\partial^2 T}{\partial z^2}\end{aligned} \tag{3}$$

The initial and boundary conditions of this problem are:

$$t\le 0: u=0,\quad v=0, w=0, T=0\quad \text{at } 0\le z\le H \tag{4}$$

$t>0$: $u=u_\infty$, $T=T_w$ at $x=0$ (channel entrance)
$t>0$: $u=-cx$, $v=0$, $T=T_w$, at $z=0$ (porous wall)
$t>0$: $u=0$,$v=0$, $T=T_w$, at $z=H$ (impermeable wall)

2.1. Final Set of Non Dimensional Governing Equations

$$\frac{\partial u'}{\partial t'}+u'\frac{\partial u'}{\partial x'}+\omega_o\frac{\partial u'}{\partial z'}=\frac{1}{Re}\left(\frac{\partial^2 u'}{\partial x'^2}+\frac{\partial^2 u'}{\partial z'^2}\right)-Xiu'-Mu'+Gr_\theta T' \tag{5}$$

$$\frac{\partial v'}{\partial t'}+u'\frac{\partial v'}{\partial x'}+\omega_o\frac{\partial v'}{\partial z'}=\frac{1}{Re}\left(\frac{\partial^2 v'}{\partial x'^2}+\frac{\partial^2 v'}{\partial z'^2}\right)-Xiv'-Mv' \tag{6}$$

$$\begin{aligned}\frac{\partial T'}{\partial t'}+u'\frac{\partial T'}{\partial x'}+\omega_o\frac{\partial T'}{\partial z'} &= \frac{1}{Re}\left[\frac{1}{Pr}\left(\frac{\partial^2 T'}{\partial x'^2}+\frac{\partial^2 T'}{\partial z'^2}\right)\right]+\\ &\quad\frac{Ec}{Re}\left[\left(\frac{\partial u'}{\partial z'}\right)^2+\left(\frac{\partial v'}{\partial z'}\right)^2\right]-\\ &\quad\frac{4}{3NPrRe}\left(\frac{\partial^2 T'}{\partial z'2}\right)+RRe\left(u'^2+v'^2\right)\end{aligned} \tag{7}$$

The initial and boundary conditions in equation (5), (6) and (7) appear as follows when transformed to their equivalent non-dimensional form:

$$t \leq 0 : u' = 0, \quad v' = 0, w' = 0, T' = 0 \quad \text{at } 0 \leq z' \leq H \tag{8}$$

$t' > 0$: $u' = 1$, $v' = 0$, $T' = 0$ at $x' = 0$ (at entry)
$t' > 0$: $u' = \frac{-CH}{U_\infty} x'$, $v' = 0$, $T' = 1$, at $z' = 0$ (contracting sheet)
$t' > 0$: $u' = 0$,$v' = 0$, $w' = 0$, $T' = 0$, at $z' = H$ (impermeable)

$$\begin{aligned} U_{i,j}^{k+1} &= [U_{i,j}^k - \frac{\Delta t}{2\Delta x} U_{i,j}^k \left(-U_{i-1,j}^{k+1} + U_{i,j}^k - U_{i-1,j}^k\right) - \frac{\omega_0 \Delta t}{2\Delta z} \left(-U_{i,j-1}^{k+1} + U_{i,j}^k - U_{i,j+1}^k\right) \\ &+ \frac{\Delta t}{2Re(\Delta x)^2} \left(U_{i+1,j}^{k+1} + U_{i-1,j}^{k+1} + U_{i+1,j}^k - 2U_{i,j}^k + U_{i-1,j}^k\right) \\ &+ \frac{\Delta t}{2Re(\Delta z)^2} \left(U_{i,j+1}^{k+1} + U_{i,j-1}^{k+1} + U_{i,j+1}^k - 2U_{i,j}^k + U_{i,j-1}^k\right) \\ &- \frac{Xi\Delta t}{2} U_{i,j}^k - \frac{M\Delta t}{2} U_{i,j}^k + \frac{\Delta t Gr_\theta}{2} \left(T_{i,j}^{k+1} + T_{i,j}^k\right)] \\ &/ \left[1 + \frac{\Delta t}{2\Delta x} U_{i,j}^k + \frac{\omega_0 \Delta t}{2\Delta z} + \frac{\Delta t}{2Re(\Delta x)^2} + \frac{\Delta t}{2Re(\Delta z)^2} + \frac{Xi\Delta t}{2} + \frac{M\Delta t}{2}\right] \end{aligned} \tag{9}$$

$$\begin{aligned} V_{i,j}^{k+1} &= [V_{i,j}^k - \frac{\Delta t}{2\Delta x} U_{i,j}^k \left(-V_{i-1,j}^{k+1} + V_{i,j}^k - V_{i-1,j}^k\right) - \frac{\omega_0 \Delta t}{2\Delta z} \left(-V_{i,j}^{k+1} + V_{i,j}^k - V_{i,j-1}^k\right) \\ &+ \frac{\Delta t}{2Re(\Delta x)^2} \left(V_{i+1,j}^{k+1} + V_{i-1,j}^{k+1} + V_{i+1,j}^k - 2V_{i,j}^k + V_{i-1,j}^k\right) \\ &+ \frac{\Delta t}{2Re(\Delta z)^2} \left(V_{i,j+1}^{k+1} + V_{i,j-1}^{k+1} + V_{i,j+1}^k - 2V_{i,j}^k + V_{i,j-1}^k\right) \\ &- \frac{Xi\Delta t}{2} V_{i,j}^k - \frac{M\Delta t}{2} V_{i,j}^k] \\ &/ \left[1 + \frac{\Delta t}{2\Delta x} U_{i,j}^k + \frac{\omega_0 \Delta t}{2\Delta z} + \frac{\Delta t}{2Re(\Delta x)^2} + \frac{\Delta t}{2Re(\Delta z)^2} + \frac{Xi\Delta t}{2} + \frac{M\Delta t}{2}\right] \end{aligned} \tag{10}$$

$$\begin{aligned} T_{i,j}^{k+1} &= [T_{i,j}^k - \frac{\Delta t}{2\Delta x} U_{i,j}^k \left(-T_{i-1,j}^{k+1} + T_{i,j}^k - T_{i-1,j}^k\right) - \frac{\Delta t \omega_0}{2\Delta z} \left(-T_{i,j-1}^{k+1} + T_{i,j}^k - T_{i,j-1}^k\right) \\ &+ \frac{\Delta t}{2PrRe(\Delta x)^2} \left(T_{i,j+1}^{k+1} + T_{i,j-1}^{k+1} + T_{i,j+1}^k - 2T_{i,j}^k + T_{i,j-1}^k\right) \\ &+ \frac{\Delta t Ec}{2PrRe(\Delta z)^2} \left(T_{i,j+1}^{k+1} + T_{i,j-1}^{k+1} + T_{i,j+1}^k - 2T_{i,j}^k + T_{i,j-1}^k\right) \\ &+ \frac{\Delta t Ec}{4Re(\Delta x)^2} \left(U_{i,j}^{k+1} - U_{i-1,j}^{k+1} + U_{i,j}^k - U_{i-1,j}^k\right)^2 \end{aligned}$$

$$+\frac{\Delta t Ec}{4Re(\Delta x)^2}\left(U_{i,j}^{k+1}-U_{i,j-1}^{k+1}+U_{i,j}^{k}-U_{i,j-1}^{k}\right)^2$$
$$-\frac{2\Delta t}{3NiPrRe(\Delta z)^2}\left(T_{i,j+1}^{k+1}+T_{i,j-1}^{k+1}+T_{i,j+1}^{k}-2T_{i,j}^{k}+T_{i,j-1}^{k}\right)$$
$$+\frac{RRe}{4}\left(U_{i,j}^{k}\right)^2+\left(V_{i,j}^{k}\right)^2$$
$$/\left[1+\frac{\Delta t}{2\Delta x}U_{i,j}^{k}+\frac{\Delta t\omega_0}{2\Delta z}+\frac{\Delta t}{PrRe(\Delta x)^2}+\frac{\Delta t}{2PrRe(\Delta z)^2}+\frac{2\Delta t}{3NiPrRe(\Delta z)^2}\right] \quad (11)$$

Subject to the initial and boundary conditions;

$t' \leq 0 : u' = 0,\ v' = 0,\ w' = 0,\ T' = 0$ at $0 \leq z' \leq H$

$t' > 0$: $u' = 1$, $v' = 0,\ T' = 0$ at $x' = 0$ (at entry)

$t' > 0$: $u' = \frac{-CH}{U_\infty}x'$, $v' = 0,\ T' = 1$, at $z' = 0$ (contracting sheet)

$t' > 0$: $u' = 0$,$v' = 0,\ w' = 0,\ T' = 0$, at $z' = H$ (impermeable)

The values of U in equation (9) are found at every nodal point for a particular i at $(k+1)^{th}$ time level. Similarly, the values of V are calculated from equation (10). The values of U and V at time $(k+1)^{th}$ time level are used to compute the values of T in equation (11) at $(k+1)^{th}$ time level. This process is repeated for all the i-levels.

The numerical calculations have been performed by fixing the mesh sizes at $\Delta x = 0.2$, $\Delta z = 0.15$ and $\Delta t = 0.0125$, where the rectangular region formed by the x-axis and z-axis has 41×41 meshes.

When the meshes are reduced and the results are compared, the results more or less agree up to the fourth decimal place. Hence the mesh size is considered appropriate for the calculation of values of the velocity and temperature. The local truncation error is of order $0(\Delta t + (\Delta x)^2 + (\Delta z)^2)$ and tends to zero as Δt,Δz and Δx tend to zero. Thus the present scheme is convergent. To ensure stability and convergence, the program is run using smaller values of Δt. It is observed that there were no significant changes in the results, which ensure the finite difference method used in the problem converge and is stable.

3. Results

The various parameters that have been varied include the magnetic parameter M, Reynold's number Re, permeability parameter Xi, radiation parameter N and time t. Two cases have been considered: When Grashof number is positive (plate cooling or heating the fluid) and when Grashof number is negative (heating plate or fluid cooling).

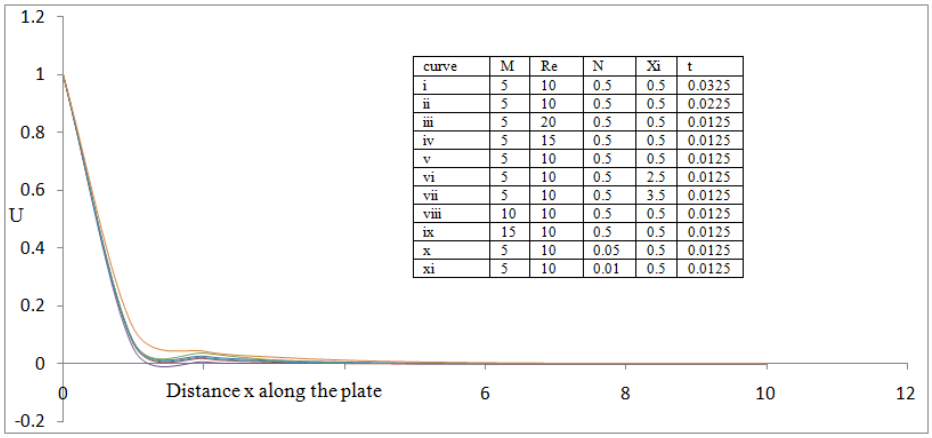

curve	M	Re	N	Xi	t
i	5	10	0.5	0.5	0.0325
ii	5	10	0.5	0.5	0.0225
iii	5	20	0.5	0.5	0.0125
iv	5	15	0.5	0.5	0.0125
v	5	10	0.5	0.5	0.0125
vi	5	10	0.5	2.5	0.0125
vii	5	10	0.5	3.5	0.0125
viii	10	10	0.5	0.5	0.0125
ix	15	10	0.5	0.5	0.0125
x	5	10	0.05	0.5	0.0125
xi	5	10	0.01	0.5	0.0125

Figure 2: Primary velocity profiles for different values when Gr_θ is positive

3.1. When Grashof Number is Positive i.e. Cooling the Sheet (Heating the Fluid)

From figure 2 its noted that increase in magnetic parameter M causes a decrease in the magnitude of both primary and the secondary velocity profiles respectively. For primary velocity profiles at $x = 2$ flow slightly reversed due to effect of contracting. From figure 4 its noted that increase in M causes a decrease in the temperature profiles. Application of a transverse magnetic field to an electrically conducting fluid give rise to a resistive type force called the Lorentz force. This force has the tendency to slow down the motion of the fluid in the boundary layer [5]. The reduced velocity by the frictional drag due to the Lorentz force is responsible for reducing thermal viscous dissipation in the fluid leading to a thinner thermal boundary layer. Magnetic field can therefore be employed to control the velocity and temperature boundary characteristics of a fluid.

From figures 2 its noted that increase in Reynolds' number *Re* causes an increase in the primary velocity profiles. From figure 3 and figure 4, increase in Reynolds's number causes increase in secondary velocity and temperature profiles respectively, but there is cross over at $x = 2.5$ cross over occur when effects of contracting is overcome by free stream. The Reynolds's number represents the ratio of the inertial to viscosity forces. Increase in Re results to a large inertial force that in turn translates to a higher velocity.

From figure 2 and 3, increase in radiation parameter *N* leads to increase in primary velocity profiles and secondary velocity profiles respectively. From figure 4 we noted that increase in *N* leads to an increase in the temperature profiles so radiation can therefore be used to control velocity and temperature boundary layers.

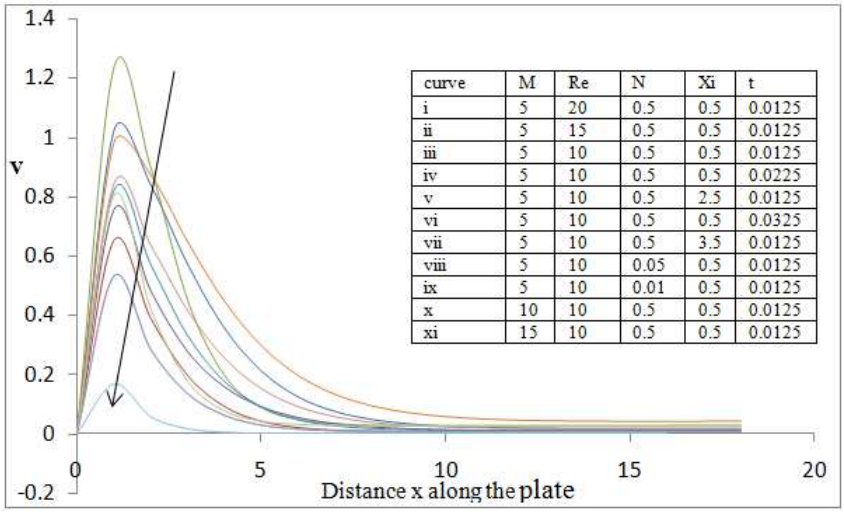

curve	M	Re	N	Xi	t
i	5	20	0.5	0.5	0.0125
ii	5	15	0.5	0.5	0.0125
iii	5	10	0.5	0.5	0.0125
iv	5	10	0.5	0.5	0.0225
v	5	10	0.5	2.5	0.0125
vi	5	10	0.5	0.5	0.0325
vii	5	10	0.5	3.5	0.0125
viii	5	10	0.05	0.5	0.0125
ix	5	10	0.01	0.5	0.0125
x	10	10	0.5	0.5	0.0125
xi	15	10	0.5	0.5	0.0125

Figure 3: Secondary profiles for different values when Gr_θ is positive

From figure 2, 3 and 4 its noted that increase in permeability Xi causes a decrease in the primary velocity, secondary velocity and temperature profiles respectively. The permeability parameter Xi is inversely proportional to the actual permeability k_p of the porous medium. Increase in Xi leads to deceleration of the flow hence the velocity decreases.

Increasingly Xi increases the resistance of the porous medium (as the permeability physically becomes less with increasing Xi). This decelerates the flow and reduces the magnitudes of both the primary and secondary velocity respectively. Thus velocity and temperature profiles can be controlled by varying the permeability of the porous medium.

From figure 2 we noted that increase in time causes increase in the primary velocity profiles. From figure 3 and figure 4 we noted that an increase in time t causes decrease in secondary velocity profiles and temperature profiles respectively near the fixed end of the contracting sheet but there is a cross over of velocity profile at around $x = 2$.

3.2. When Grashof Number is Negative i.e. Heating the Sheet (Cooling the Fluid)

From figure 5 and 6 it is noted that increase in magnetic parameter M causes a decrease in the magnitude of both primary and the secondary velocity profiles respectively. From figure 7 we noted that increase in M causes a decrease in the temperature profiles. Application of a transverse magnetic field to an electrically conducting fluid give rise to a resistive type force called the Lorentz Force. This force has the tendency to slow

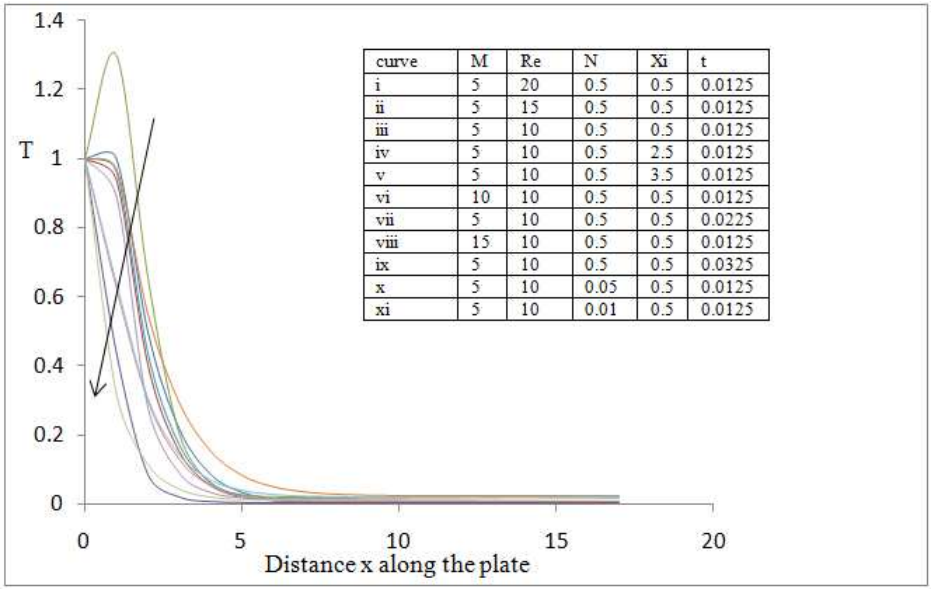

curve	M	Re	N	Xi	t
i	5	20	0.5	0.5	0.0125
ii	5	15	0.5	0.5	0.0125
iii	5	10	0.5	0.5	0.0125
iv	5	10	0.5	2.5	0.0125
v	5	10	0.5	3.5	0.0125
vi	10	10	0.5	0.5	0.0125
vii	5	10	0.5	0.5	0.0225
viii	15	10	0.5	0.5	0.0125
ix	5	10	0.5	0.5	0.0325
x	5	10	0.05	0.5	0.0125
xi	5	10	0.01	0.5	0.0125

Figure 4: Temperature profiles for different values when Gr_θ is positive

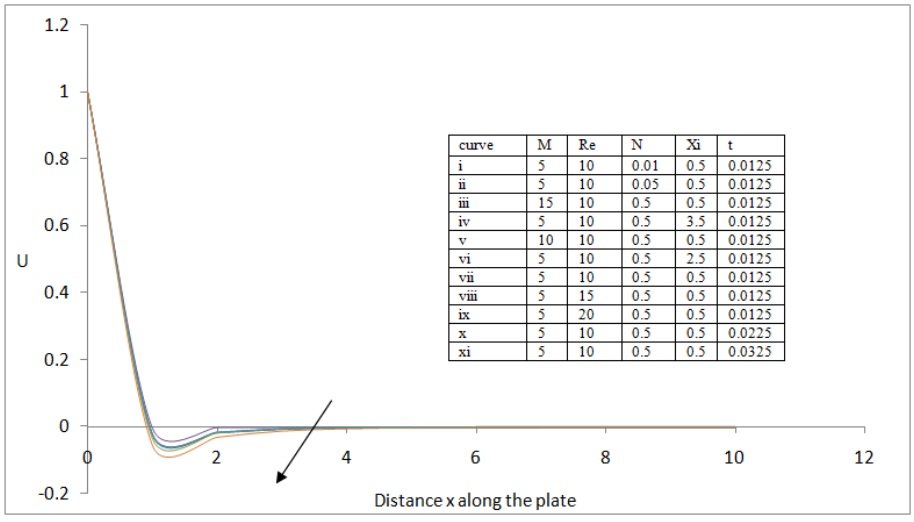

curve	M	Re	N	Xi	t
i	5	10	0.01	0.5	0.0125
ii	5	10	0.05	0.5	0.0125
iii	15	10	0.5	0.5	0.0125
iv	5	10	0.5	3.5	0.0125
v	10	10	0.5	0.5	0.0125
vi	5	10	0.5	2.5	0.0125
vii	5	10	0.5	0.5	0.0125
viii	5	15	0.5	0.5	0.0125
ix	5	20	0.5	0.5	0.0125
x	5	10	0.5	0.5	0.0225
xi	5	10	0.5	0.5	0.0325

Figure 5: Primary velocity profiles for different values when Gr_θ is negative

down the motion of the fluid in the boundary layer [5]. The reduced velocity by the frictional drag due to the Lorentz force is responsible for reducing thermal viscous dissipation in the fluid leading to a thinner thermal boundary layer. Magnetic field can

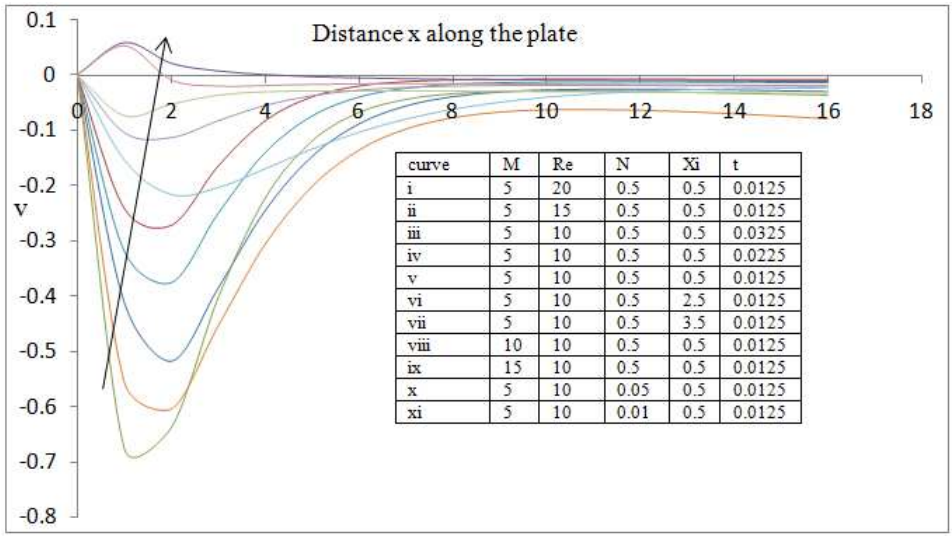

curve	M	Re	N	Xi	t
i	5	20	0.5	0.5	0.0125
ii	5	15	0.5	0.5	0.0125
iii	5	10	0.5	0.5	0.0325
iv	5	10	0.5	0.5	0.0225
v	5	10	0.5	0.5	0.0125
vi	5	10	0.5	2.5	0.0125
vii	5	10	0.5	3.5	0.0125
viii	10	10	0.5	0.5	0.0125
ix	15	10	0.5	0.5	0.0125
x	5	10	0.05	0.5	0.0125
xi	5	10	0.01	0.5	0.0125

Figure 6: Secondary velocity profiles for different values when Gr_θ is negative

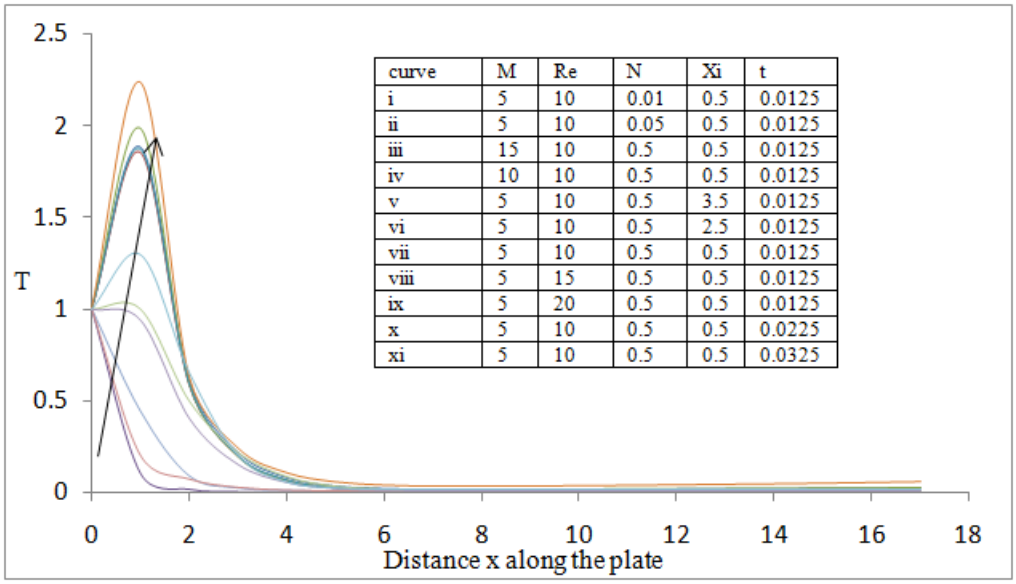

curve	M	Re	N	Xi	t
i	5	10	0.01	0.5	0.0125
ii	5	10	0.05	0.5	0.0125
iii	15	10	0.5	0.5	0.0125
iv	10	10	0.5	0.5	0.0125
v	5	10	0.5	3.5	0.0125
vi	5	10	0.5	2.5	0.0125
vii	5	10	0.5	0.5	0.0125
viii	5	15	0.5	0.5	0.0125
ix	5	20	0.5	0.5	0.0125
x	5	10	0.5	0.5	0.0225
xi	5	10	0.5	0.5	0.0325

Figure 7: Temperature profiles for different values when Rr_θ is negative

therefore be employed to control the velocity and temperature boundary characteristics

of a fluid.

From figures 5 and 7 it is noted that increase in Reynolds' number *Re* causes an increase in the primary and temperature profiles respectively. From figure 6 its noted that increase in Reynolds's leads to an increase in secondary velocity profiles but there is a cross over at $x = 2.5$. The Reynolds's number represents the ratio of the inertial to viscosity forces. Increase in *Re* results to a large inertial force that in turn translate to a higher velocity.

From figure 5 and 6 it is noted that increase in radiation parameter N leads to increase in primary velocity profiles and secondary velocity profiles respectively. From figure 7 we noted that increase in N leads to an increase in the temperature profiles so radiation can therefore be used to control velocity and temperature boundary layers.

From figure 5, 6 and 7 its noted that increase in permeability Xi, Causes a decrease in the primary velocity, secondary velocity and temperature profiles respectively The permeability parameter Xi is inversely proportional to the actual permeability k_p of the porous medium. Increase in Xi leads to deceleration of the flow hence the velocity decreases. Increasingly Xi increases the resistance of the porous medium (as the permeability physically becomes less with increasing Xi). This decelerates the flow and reduces the magnitudes of both the primary and secondary velocities respectively. This velocity and temperature profile can be controlled by varying the permeability of the porous medium.

From figure 5 and 6 its noted that increase in time causes increase in the primary velocity and secondary velocity profiles respectively. From figure 7 we noted increase in time leads to increase in temperature profiles.

4. Conclusion

The analysis of various parameters on unsteady laminar boundary layer flow of an incompressible, electrically conducting, and viscous Newtonian fluid past contracting electrically non-conducting sheet embedded in porous media has been carried out. The numerical solutions of velocity and temperature fields are obtained by finite difference method with Crank Nicolson approximation. [5] analyzed effects of magnetic parameter, injection parameter, Schmidt number, radiation parameter, viscous stress, Eckert number, Dufour number, Soret number, Reynolds number, Nusset number, rotation and porosity on stretching sheet. The problem at hand has contracting sheet. In order to validate the present results, the boundary condition for the sheet is changed so as to reflect stretching. The results are compared with those of [5] and agree. The main conclusions are as follow:

1. Primary velocity profiles, secondary velocity profiles and temperature profiles

decreases with increase in magnetic parameter M, for both cooling and heating of the sheet

2. Increase in Reynolds number Re leads to increase in primary velocity profiles, secondary velocity profiles and temperature profiles.

3. Increase in radiation parameter N leads to increase in primary velocity profiles, secondary velocity profiles and temperature profiles.

4. Increase in permeability parameters Xi leads to decrease in primary velocity profiles, secondary velocity profiles and temperature profiles.

5. Increase in time leads to increase in primary velocity profiles, secondary velocity profiles and temperature profiles. For both cooling and heating of the sheet.

Thus varying magnetic parameter M, Reynolds' number Re, radiation parameter N, permeability parameter Xi and time t can be used to control the growth of velocity boundary layer and thermal boundary layer.

Acknowledgment

The authors are thankful to the NACOSTI, National Commission for Science, Technology and Innovation Kenya for the financial support.

References

[1] Ahmed, N., Kalita, H., and Barua, D. (2010). Unsteady mhd free convective flow past a vertical porous plate immersed in a porous media with hall current, thermal diffusion and heat source. *International Journal of Engineering, Science And Technology*, 2(6):59–97.

[2] Bhattacharyya, K. (2011). Effects of heat source/sink on mhd flow and heat transfer over a shrinking sheet with mass suction. *Chemical Engineering Research Bulletin*, 15:12–17.

[3] Dawood, A. and Hmood, B. (2006). Steady free convection through porous media enclosing a rectangular isothermal body. *Al-Rafidain Engineering*, 14(1).

[4] et al., V. (1986). Buoyancy effect on mhd flow past a permeable bed. *Dcf Science Journal*, 36:295–314.

[5] Giterere, K., Kinyanjui, M., and Uppal, S. (2012). Mhd flow in porous media over stretching surface in a rotating system with heat and mass transfer. *International Journal of Pure and Applied Mathematics*, 4:9–32.

[6] Gupta, A. and Gupta, P. (1977). Heat and mass transfer on a stretching sheet with suction or blowing. *Canadian Journal of Chemical Engineering*, 55:744.

[7] Hayat, T. A., Javed, T., and Sajid, M. (2007). Three dimensional rotating flow induced by a shrinking sheet for suction. *Chaos, solitons and Fra et al*, 39:1615–1626.

[8] Kinyanjui, M., Kwanza, J., and Uppal, S. (2001). Mhd free convection heat and mass transfer of a heat generating fluid past an impulsively started infinite vertical porous plate with hall current and radiation absorption. *Energy Conversion and Management*, 42:917–931.

[9] Kishore, P., Rajessh, V., and Varma, S. V. K. (2010). The effects of thermal radiation and viscous dissipation on mhd heat and mass diffusion flow past a surface embedded in a porous medium. *International Journal of Applied Mathematics and Mechanics*, 6(11):79–97.

[10] Neeraja, V. E. and Babu, G. S. (2013). Hall effects on mhd convective flow through a medium in a rotating parallel plate channel. *Asian Journal of Current Engineering And Mathematics*, 2:181–189.

[11] Raptis, A., Tzivanidis, G., and Kafousias, N. (1981). Free convection and mass transfers flow through a porous medium bounded by an infinite vertical limiting surface constant suction. *Letter of Heat and mass transfer*, 8:417.

[12] Saritha, S. and Narayana, P. S. (2012). Thermal diffusion and chemical reaction effects on unsteady mhd free convection flow past a semi infinite vertical permeable moving plate. *Asian Journal of Current Engineering and Mathematics*, 2:131–138.

[13] Seethamahalakshim, B. N. and Prasad, G. (2012). Mhd free convective mass transfer flow past an infinite vertical porous plate with variable suction and soret effect. *Asian Journal of Current Engineering and Mathematics*, 3:49–55.

[14] Subhas, A., Joshi, A., and Sonth, R. (2001). Heat transfer in mhd visco-elastic fluid flow over a streching surface. *Journal of Applied Mathematics and Mechanics*, 81(10):691–698.

[15] Vidyasagar and Ramana, B. (2013). Radiation effects on mhd free convective flow of krushinshiki fluid with mass transfer past a vertical porous plate through porous media. *Asian Journal of Current Engineering and Mathematics*, 2:170–174.

[16] Yamamoto, K. and Iwamura, N. (1976). Flow with convective acceleration through a porous medium. *Journal of Current Engineering Mathematics*, 10:41–54.